Rheological Properties of Nanofiltered Athabasca Bitumen and Maya Crude Oil

ARTICLE *in* ENERGY & FUELS · AUGUST 2009

Impact Factor: 2.79 · DOI: 10.1021/ef900313r

4 AUTHORS, INCLUDING:

MD Anwarul Hasan
American University of Beirut
27 PUBLICATIONS **304** CITATIONS
SEE PROFILE

Michal Fulem
University of Chemistry and Technology, Pra…
61 PUBLICATIONS **601** CITATIONS
SEE PROFILE

Energy Fuels **XXXX,** *XXX,* 000–000 · DOI:10.1021/ef900313r

energy&fuels
article

Rheological Properties of Nanofiltered Athabasca Bitumen and Maya Crude Oil

Anwarul HasanMD,[†] Michal Fulem,[‡,§,¶] Ala Bazyleva,[‡] and John M. Shaw*[,‡]

[†]*Department of Mechanical Engineering, University of Alberta, Edmonton, Alberta, T6G 2G8, Canada,* [‡]*Department of Chemical and Materials Engineering, University of Alberta, Edmonton, Alberta T6G 2G6, Canada,* [§]*Department of Physical Chemistry, Institute of Chemical Technology, Prague, Technická 5, CZ-166 28 Prague 6, Czech Republic, and* [¶]*Institute of Physics, Academy of Sciences of the Czech Republic, v.v.i., Cukrovarnická 10, CZ-162 53 Prague 6, Czech Republic*

Received April 8, 2009. Revised Manuscript Received July 4, 2009

Complex viscosities of Athabasca bitumen (Alberta, Canada) and Maya crude oil (Mexico) samples, along with their permeates and retentates obtained by nanofiltration at 473 K through 5-, 10-, 20-, 50-, and 200-nm ceramic membranes, were investigated over the temperature interval of 298−373 K. The pentane−asphaltene content of the samples varied from 1.5 wt % to 57.2 wt %, whereas the asphaltene-free composition of the samples did not vary from the feed composition (within experimental error). At temperatures of < 323 K, part of the maltenes of both of these hydrocarbon resources is solid. The solid maltene fraction is a function of temperature. If this additional solid is taken into account, the experimental relative viscosities for both Athabasca bitumen- and Maya crude-related samples fall on a single master curve, over the entire temperature interval, irrespective of the asphaltene content. The rheological behavior of all feed, permeate, and retentate samples is consistent with that of a slurry that is comprised of a Newtonian liquid plus a dispersed solid that is comprised of noninteracting hard spheres, where the solids fraction is the sum of the solid maltene plus asphaltene mass fractions. Failure to account for solid maltenes in the interpretation of rheological data for these hydrocarbon resources leads to misattributions related to the nature and importance of the role that asphaltenes play in the determination of the complex viscosity of these hydrocarbon resources.

Introduction

Bitumen and heavy oils are asphaltene-rich complex hydrocarbon mixtures that pose numerous challenges during production, transport, and refining.[1,2] The high viscosity of these hydrocarbon resources is a key processing determinant that is frequently attributed to their asphaltene content and to asphaltene−maltene interactions. For example, Mack et al.[3] showed that the viscosity of a deasphalted oil was up to several hundred times lower than the viscosity of mixtures that are comprised of up to 20 vol % asphaltenes + parent oil. Moreover, asphaltenes flocculate, aggregate, and sediment,[2,4,5] even in aromatic solvents such as toluene, at concentrations as low as 100 mg/L.[6] Aggregation is linked to various processing problems, from formation damage and well plugging[7] to reactor and line coking to distillation tower plugging[8−14] to catalyst deactivation.[15] An improved understanding of asphaltenes, and their influence on the properties of bitumen and heavy oils, would help solve many of these problems[16] and would facilitate the development of more-efficient processes for the production, transport, and refining of these important hydrocarbon resources.[17]

The viscosity of bitumen and heavy oil is a key process variable for which data are available.[18] However, most of the available data focus on the dependence of viscosity on external factors such as pressure, temperature, and the presence of various additives, e.g., diluents (benzene, toluene, *n*-decane, etc.) and dissolved gases (CO_2, N_2, CH_4, C_2H_6, etc). A few studies also consider the shear rate dependence of viscosity.[18,19]

*Author to whom correspondence should be addressed. E-mail address: jmshaw@ualberta.ca.

(1) Mazza, A. G. *Modelling of the liquid-phase thermal cracking kinetics of Athabasca bitumen and its major chemical fractions*, Ph.D. Thesis, University of Toronto, Toronto, Canada, 1987.
(2) Branco, V. A. M.; Mansoori, G. A.; De Almeida Xavier, L. C.; Park, S. J.; Manafi, H. J. *Pet. Sci. Eng.* **2001**, *32* (2−4), 217.
(3) Mack, C. *J. Phys. Chem.* **1932**, *36*, 2901.
(4) Murgich, J.; Strausz, O. P. *Pet. Sci. Technol.* **2001**, *19* (1−2), 231.
(5) Yarranton, H. W. *J. Dispersion Sci. Technol.* **2005**, *26* (1), 5.
(6) Andreatta, G.; Bostrom, N.; Mullins, O. C. *Langmuir* **2005**, *21* (7), 2728.
(7) Priyanto, S.; Mansoori, G. A.; Suwono, A. *Chem. Eng. Sci.* **2001**, *56* (24), 6933.
(8) Taylor, R. S.; Stemler, P. S.; Lemieux, A.; Fyten, G. C.; Cheng, A. In *Proceedings of the 7th Canadian International Petroleum Conference*, Calgary, Alberta, Canada, 2006; Paper 053.
(9) Licha, P. M.; Herrera, L. *Soc. Pet. Eng. J.* **1975**, Paper 5304.
(10) Escobedo, J.; Mansoori, G. A. *SPE Prod. Facil.* **1997**, (May), 116.
(11) Holder, G. D.; Enick, R. M.; Mohamed, R. S. *Fluid Phase Equilib.* **1996**, *117*, 126.
(12) Sharma, M. M.; Yen, T. F.; Chiligar, G. V.; Donaldson, E. C. In *Enhanced Oil Recovery, Vol. 1: Fundamentals and Analyses*; Development in Petroleum Science; Elsevier: New York, 1985; p 223.
(13) Licha, M. P. *Oil Sands* **1977**, 609.
(14) Jacobs, I. C.; Thorne, M. A. *Soc. Pet. Eng. J.* **1986**, Paper 14823.
(15) Sheu, E. Y. *Energy Fuels* **2002**, *16* (1), 74.
(16) Mohamed, R. S.; Ramos, A. C. S.; Loh, W. *Energy Fuels* **1999**, *13* (2), 323.
(17) Baltus, R. E. Characterization of Asphaltenes and Heavy Oils Using Hydrodynamic Property Measurements. In *Structures and Dynamics of Asphaltenes*; Mullins, O. C., Sheu, E. Y., Eds.; Plenum Press: New York and London, 1998; p 303.
(18) Seyer, F. A.; Gyte, G. W. In *AOSTRA Technical Handbook on Oil Sands, Bitumens and Heavy Oils*; AOSTRA Technical Publications: Alberta, Canada, 1989; Chapter 4.
(19) Briggs, J. P. *The Measurements of Bitumen Viscosity at Shear Rates, Temperatures and Pressures Which Approximate to Reservoir Conditions*; Alberta Research Council: Edmonton, Alberta, Canada, June 1978.

Reported viscosity data[19−30] were obtained using various viscometers such as capillary-flow, rotating-cylinder, cone-and-plate, and rolling-ball viscometers. In the case of rotational viscometers, the steady shear mode was used for almost all measurements.[25−28] The impact of viscosity measurement techniques on the values of viscosity obtained is discussed in detail elsewhere.[31]

Investigations on the influence of asphaltenes on hydrocarbon resource viscosity have focused on model mixtures where chemically separated (solvent extracted) asphaltenes are added to standard organic solvents or to deasphalted oil (maltenes) to obtain samples with a range of asphaltene concentrations.[32]

The aggregation of asphaltenes in various solvents has also been studied.[7,15,33−35] Bouhadda et al.[33] found that aggregated asphaltene particles in toluene appear spherical for concentrations up to 15 vol % and have an aggregation number of ∼5. The results by Lorenz et al.[36] suggest that asphaltenes appear to be almost spherical and nonsolvated in mixtures with kerosene, gas oil, benzene, and decalin, as well as in various lighter fractions of crude oil obtained through ultracentrifugation for concentrations in the range of 1−2 wt %. Reerink[37] modeled asphaltene aggregates as oblate ellipsoids with a minor axis of ∼1 nm and a major axis of ∼5−9 nm and computed intrinsic viscosities in the range of 5−8 (where a value of 2.5 is consistent with rigid hard spheres). Using small-angle neutron scattering, Gawrys and Kilpatrick[38] showed that asphaltenes in mixed (toluene + methanol) or (toluene + heptane) solutions aggregate to form oblate cylinders. Takeshige[34] suggested that asphaltenes in benzene consist of double layers with semi-axes of 3.19, 1.05, and 0.36 nm. Priyanto et al.[7] observed two distinct points of sharp changes of slope in graphs of relative viscosity versus asphaltene concentration, which they attributed to micellization phenomena. In a series of studies conducted at the Texaco Research Center,[39−44] asphaltenes obtained from five different sources yielded very similar rheological behavior, indicating that the effect of shape and extent of solvation for those materials were quite similar. There is little agreement in the literature, other than that asphaltenes appear to be particulate!

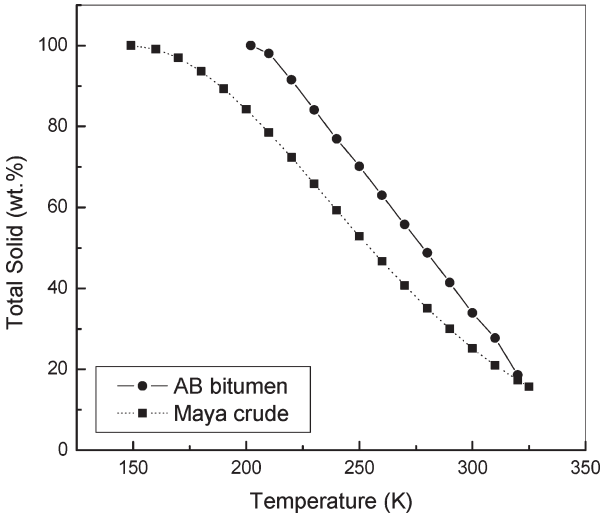

Figure 1. Total solids content (wt %) for Athabasca bitumen and Maya crude oil.

The phase behavior of heavy oils, apart from asphaltenes, is also complex. For example, Athabasca bitumen and Maya crude oil both comprise a minimum of three phases at 300 K: solid asphaltenes, liquid maltenes, and solid maltenes. The phase behaviors of Maya crude oil[45] and Athabasca bitumen[46] are addressed in detail elsewhere. A key attribute relevant to the interpretation of rheological data presented here is that the maltenes of these feeds solidify (see Figure 1).

The hypothesis tested in this work is whether taking into account the phase behavior of the maltenes, neglected in prior research, can reduce the ambiguity in the interpretation of the rheological behavior of asphaltenes in hydrocarbon resources. For example, Maya crude is comprised of 15.7 wt % pentane-insoluble asphaltenes. At 283 K, ∼18 wt % of the maltene fraction is also solid, whereas at 325 K, the maltene fraction is liquid.[45] Without prior knowledge of this significant change in phase behavior, the rheological behavior and changes in rheological behavior in this temperature interval can be misinterpreted and misattributed. In this contribution, the rheological behavior of Athabasca bitumen and Maya crude oil, along with their permeates and retentates obtained by

(20) Briggs, J. P. *Summary of Viscosity Measurements Data Obtained during February and March 1978*; Alberta Research Council: Edmonton, Alberta, Canada, April 1978.
(21) Camp, F. W., Ed. *The Tar Sands of Alberta, Canada*; 2nd Edition; Cameron Engineers, Inc.: Denver, CO, 1974; p 23.
(22) Charbonnier, R. P.; Draper, R. G.; Harper, W. H.; Yates, A. *Analyses and Characteristics of Oil Samples from Alberta*; Information Circular 232; Canada Department of Energy Mines and Resources, Mine Branch: Ottawa, Canada, 1969; pp 182−184.
(23) Dealy, J. M. *Can. J. Chem. Eng.* **1979**, *57*, 677.
(24) Ward, S. H.; Clark, K. A. *Determination of the Viscosities and Specific Gravities of the Oils in Samples of Athabasca Bituminous Sand*; Report 57; Research Council of Alberta: Edmonton, Canada, 1950.
(25) Flock, D. L.; Boogmans, T. *A Laboratory Investigation of Steam Solvent Extraction of Heavy Oils and Bitumen for In-Situ Application: Final Report on AOSTRA Research Agreement 8*; March 1978.
(26) Jacobs, F. A. *Viscosity of carbon dioxide saturated Athabasca bitumen*, M.Sc. Thesis, University of Calgary, Calgary, Canada, 1978.
(27) Mehrotra, A. K.; Svrcek, W. Y. *AOSTRA J. Res.* **1985**, *1* (4), 263.
(28) Svrcek, W. Y.; Donnelly, J. K.; Stanislav, J. *Measurement, Correlation and Prediction of Oil Sand Hydrocarbons: Final Report on AOSTRA Research Agreement 13*; June 1979.
(29) Robinson, D. B.; Sim, S.-K.; Chen C.-J. *The Behavior of Bitumen Mixtures during In-Situ Recovery: Final Report on AOSTRA Research Agreement 184*; July 1983.
(30) Schramm, L. L.; Kwak, J. C. T. J. *Can. Pet. Technol.* **1988**, *27* (Feb.), 26.
(31) Bazyleva, A. B.; Hasan, A.; Fulem, M.; Becerra, M.; Shaw, J. M. *Bitumen and Heavy Oil Rheological Properties—Reconcilliation with Viscosity Measurements*. Presented at PETROPHASE, June 14−18, 2009, Rio de Janiero, Brazil. (To be submitted for publication, 2009.)
(32) Marques, J. *Hydrocraquage Catalytique Des Asphaltenes Pour L'Hydrotraitement De Residus En Lit Fixe*, Ph.D. Thesis, Docteur De L'Universite De Poitiers, Lyon, France, 2006.
(33) Bouhadda, Y.; Bendedouch, D.; Sheu, E.; Krallafa, A. *Energy Fuels* **2000**, *14* (4), 845.
(34) Takeshige, W. *J. Colloid Interface Sci.* **2001**, *234* (2), 261.
(35) Mostowfi, F.; Indo, K.; Mullins, O. C.; McFarlane, R. *Energy Fuels* **2009**, *23*, 1194.
(36) Lorenz, P. B.; Bolen, R. J.; Dunning, H. J.; Eldib, I. A. *J. Colloid Sci.* **1961**, *16*, 493.
(37) Reerink, H. *Ind. Eng. Chem. Prod. Res. Develop.* **1973**, *12*, 82.
(38) Gawrys, K. L.; Kilpatrick, P. K. *J. Colloid Interface Sci.* **2005**, *288* (2), 325.
(39) Storm, D. A.; Baressi, R. J.; Sheu, E. Y. *Energy Fuels* **1995**, *9* (1), 168.
(40) Sheu, E. Y.; Shields, M. B.; Storm, D. A. *Fuel* **1994**, *73* (11), 1766.
(41) Storm, D. A.; Sheu, E. Y. *Fuel* **1993**, *72* (2), 233.
(42) Sheu, E. Y.; De Tar, M. M.; Storm, D. A. *Fuel* **1991**, *70* (10), 1151.
(43) Storm, D. A.; Barresi, R. J.; DeCanio, S. J. *Fuel* **1991**, *70* (6), 779.
(44) Storm, D. A.; Sheu, E. Y.; DeTar, M. M.; Barresi, R. J. *Energy Fuels* **1994**, *8*, 567.
(45) Fulem, M.; Becerra, M.; Hasan, M. A.; Zhao, B.; Shaw, J. M. *Fluid Phase Equilib.* **2008**, *272* (1−2), 32.
(46) Hasan, M. A.; Fulem, M.; Becerra, M.; Zhao, B.; Shaw, J. M. *Phase behaviour of Athabasca bitumen based on calorimetry and rheometry*. To be submitted for publication, 2009.

Table 1. SARA Analysis of Athabasca Bitumen-Derived Samples[a]

	Amount (wt %)					
component	ABP10	ABP20	ABP50	AB	ABR200	ABR10
saturates	18.9 (20)[b]	18.4 (21)[b]	17.1 (20)[b]	16.1 (20)[b]	9.4 (20)[b]	8.9 (21)[b]
aromatics	56.7 (60)[b]	53.0 (59)[b]	53.4 (62)[b]	48.5 (60)[b]	26.0 (52)[b]	25.4 (59)[b]
resins	19.1 (20)[b]	18.2 (20)[b]	15.9 (18)[b]	16.8 (21)[b]	14.6 (29)[b]	8.7 (20)[b]
asphaltenes (C5)	5.3	10.4	13.6	18.6	50.0	57.2

[a] ABP10: Athabasca bitumen, 10 nm permeate; ABR10: Athabasca bitumen, 10 nm retentate; ABP20: Athabasca bitumen, 20 nm permeate; ABR200: Athabasca bitumen, 200 nm retentate; ABP50: Athabasca bitumen, 50 nm permeate. [b] Data shown in parentheses are given on an asphaltene-free basis (wt %).

Table 2. SARA Analysis of Maya Crude Oil-Derived Samples[a]

	Amount (wt %)					
component	MP5	MP10	MP20	MP50	Maya crude	MR5
saturates	39.6 (40)[b]	34.4 (37)[b]	34.1 (37)[b]	31.7 (35)[b]	31.6 (38)[b]	16.9 (32)[b]
aromatics	46.7 (47)[b]	43.7 (47)[b]	43.1 (47)[b]	47.1 (52)[b]	42.5 (51)[b]	26.4 (50)[b]
resins	12.3 (12)[b]	15.7 (17)[b]	14.8 (16)[b]	11.8 (13)[b]	10.2 (12)[b]	10.0 (19)[b]
asphaltenes (C5)	1.5	6.2	8.1	9.4	15.7	46.7

[a] MP5: Maya, 5 nm permeate; MP10: Maya, 10 nm permeate; MP20: Maya, 20 nm permeate; MP50: Maya, 50 nm permeate; MR5: Maya, 5 nm retentate. [b] Data shown in parentheses are given on an asphaltene-free basis (wt %).

solvent-free nanofiltration,[47] are investigated. The results obtained are interpreted in light of the underlying phase behavior of these samples and the theory related to the rheology of dispersions.

Rheological Response of Dispersions

A detailed review of the rheology of dispersions is beyond the scope of the present work. Readers are referred elsewhere.[48−52] For a dispersion of noninteracting uniform rigid spherical particles in a Newtonian fluid, relative viscosity can be predicted using various hard-sphere models.[50−52] As the size, shape, size distribution, surface texture, of asphaltene particles and aggregates deviate from those of an ideal hard sphere, the relative viscosity of dispersions changes accordingly. Numerous empirical and semiempirical models have been proposed to account for specific cases.[50−52] However, Sudduth[53] showed that many of these equations can be reduced to a single generalized form:

$$\ln\left(\frac{\eta}{\eta_0}\right) = \left(\frac{[\eta]}{k}\right)\left(\frac{1}{\sigma - 1}\right)[(1 - k\varphi)^{1-\sigma} - 1] \qquad (1)$$

where η is the viscosity of dispersion, η_o the viscosity of the continuous phase, $[\eta]$ the intrinsic viscosity, φ the volume fraction of particles, k the crowding factor (it takes into account the reduction of available volume due to crowding of particles as the volume fraction of solids increase), and σ the particle interaction coefficient. In this paper, the generalized Sudduth equation (eq 1) is used to interpret rheological data. This equation describes the behavior of Newtonian and non-Newtonian suspensions alike. The values of parameters are linked directly to fluid and particle physics theory. For example, the intrinsic viscosity $[\eta]$ for a slurry of spherical particles dispersed in a Newtonian fluid is 2.5; $\sigma = 3.5$ for noninteracting hard spheres, and $1 < k < 2$. Furthermore, eq 1 is a generalized form for numerous rheological models.

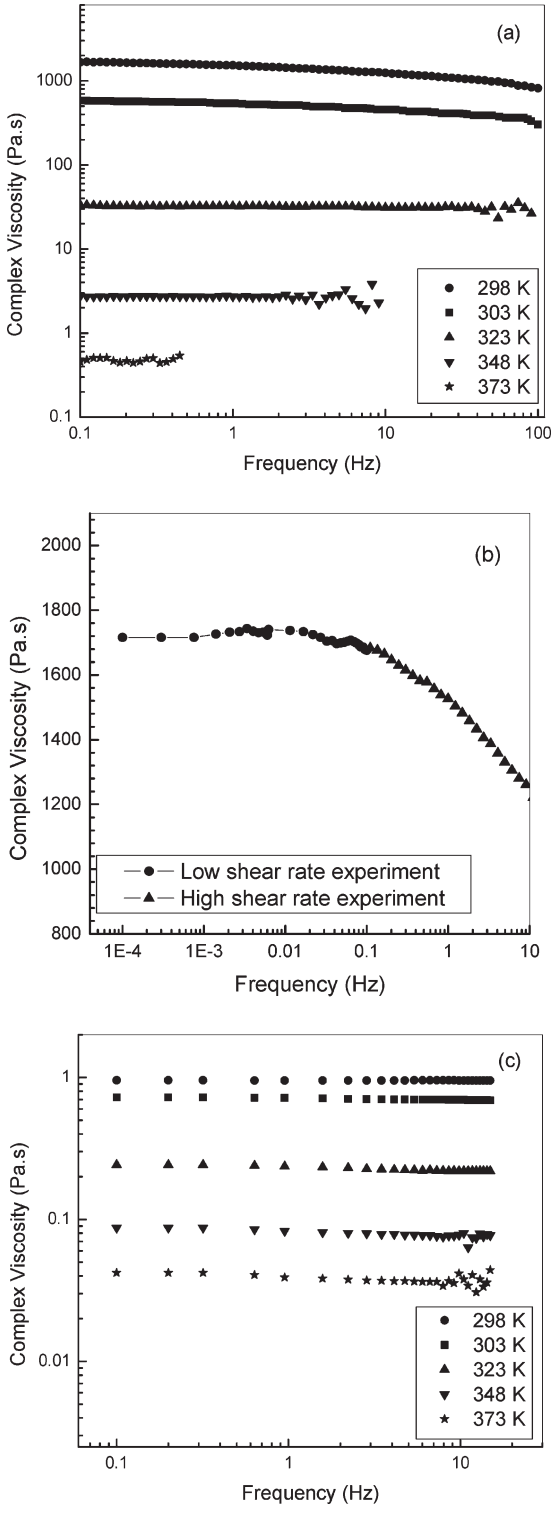

Figure 2. Complex viscosity for (a) Athabasca bitumen summary, (b) Athabasca bitumen low-frequency measurements at 298 K, and (c) Maya crude oil summary.

(47) Zhao, B.; Shaw, J. M. *Energy Fuels* **2007**, *21* (5), 2795.
(48) Einstein, A. *Ann. Phys.* **1906**, *19* (2), 289.
(49) Einstein, A. *Ann. Phys.* **1911**, *34* (3), 591.
(50) Batchelor, G. K. *J. Fluid Mech.* **1970**, *41* (3), 21.
(51) Batchelor, G. K. *J. Fluid Mech.* **1977**, *83* (Nov), 21.
(52) Batchelor, G. K.; Green, J. T. *J. Fluid Mech.* **1972**, *56* (3), 401.
(53) Sudduth, R. D. *J. Appl. Polym. Sci.* **1993**, *48* (1), 25.

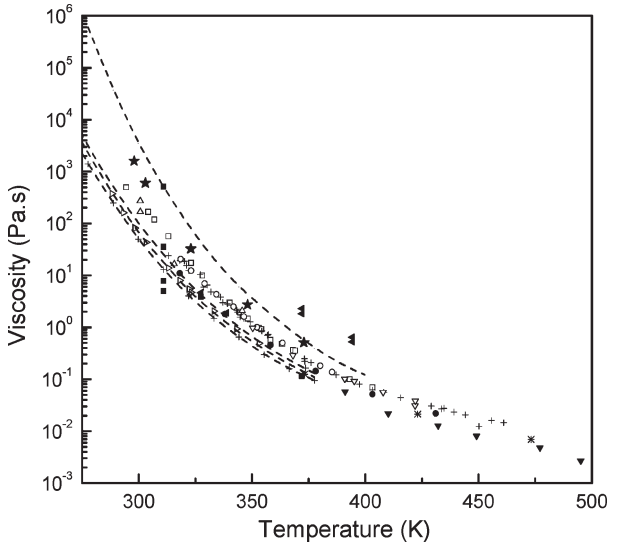

Figure 3. Comparison between the zero shear complex viscosity values for Athabasca bitumen obtained in this study with apparent viscosities of other studies in the literature. (Graphic legend: (★) this work, PPR, zero shear rate; (▼) refs 19 and 20, RBV, $\gamma' = 14-225\ s^{-1}$; (▽) refs 19 and 20, CCV, $\gamma' = 12-1400\ s^{-1}$; (■) ref 21, from different locations, method and γ' value not stated; (△) ref 23, MS, $\gamma' = 1\ s^{-1}$; (- - -) ref 24, from different locations, CapV, γ' value not stated; (◆) ref 25, CCV, $\gamma' = 13-2300\ s^{-1}$; (□) ref 26, CCV, γ' value not stated; (○) ref 27, CCV, γ' value not stated; (+) ref 28, CCV, γ' value not stated; and (∗) ref 29, CapV, γ' value not stated. Data denoted by a solid left-pointing triangle represent data obtained from ref 22 (method and γ' value were not stated). Data denoted by an open right-pointing triangle represent data obtained from ref 30 (CCV, $\gamma' = 460\ s^{-1}$). Abbreviations and symbols: PPR, parallel-plate rheometer; RBV, rolling-ball viscometer; CCV, concentric-cylinder viscometer; MS, mechanical spectrometer; CapV, capillary viscometer; γ', shear rate; and ω, angular frequency (equivalent to shear rate).)

For example, if $\sigma = 0$, 1, or 2, eq 1 becomes the Arrhenius, Krieger−Dougherty, or Mooney equation, respectively. To make the best use of the theory related to relative viscosity, the volume or mass fraction of dispersed species in the crude and bitumen samples must be known accurately, and the liquid composition should be invariant. These aspects are both challenging, because the solids mass fraction of the maltene varies with temperature. Hence, the solid-free liquid composition varies with temperature, as does the average density of particles. The viscosity of the solid-free continuous medium must be obtained by extrapolating experimental viscosity data to zero solids.

Experimental Section

Materials. The Athabasca bitumen and Maya crude oil samples, along with permeates and retentates obtained from nanofiltration experiments, were available from a prior study,[47] where the apparatus, sample preparation, and analysis procedures are described in detail. Saturates, aromatics, resins, and asphaltenes (SARA) analyses are given in Tables 1 and 2, for the sake of convenience. For chemically separated maltenes, *n*-pentane was added to bitumen/crude oil at a solvent: oil ratio of 40:1. The solution was stirred overnight at room temperature and then filtered in two steps via vacuum filtration, using a Fisher Q2 brand filter paper, with a pore size of 1−5 μm, and then a 0.22-μm Millipore membrane (mixed cellulose ester). The filtration membranes and the flask were washed with small volumes of *n*-pentane to eliminate residual oil. This step was repeated until the filtrate was colorless. The permeate was distilled to separate solvent from the maltenes.

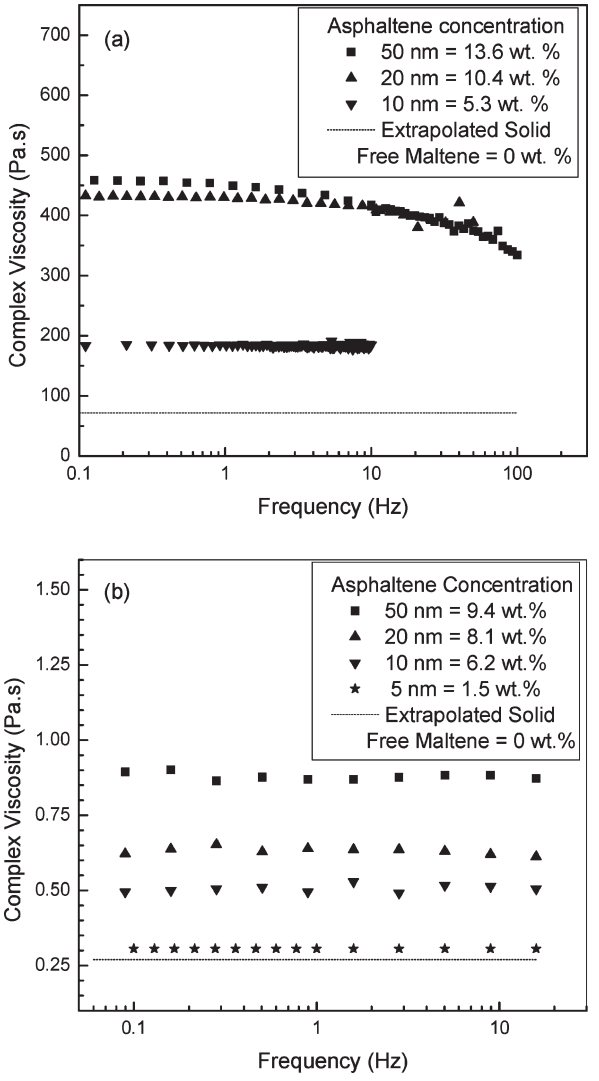

Figure 4. Complex viscosity for nanofiltered-permeate samples at 298 K: (a) Athabasca bitumen and (b) Maya crude oil.

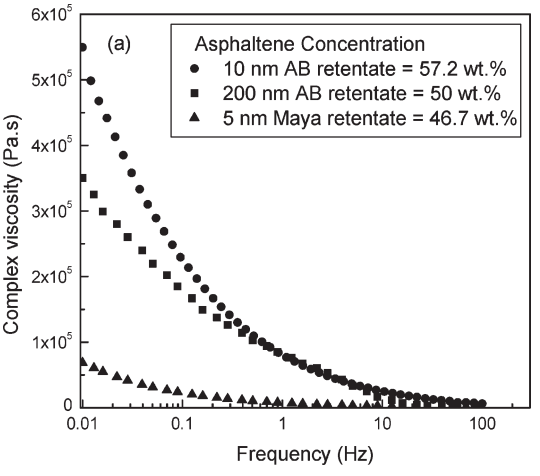

Figure 5. Complex viscosity values for Athabasca bitumen and Maya crude oil retentates at 323 K.

Rheology Measurements. Complex viscosity measurements were conducted using a Bohlin Gemini 200 HR Nano-Rheometer (Malvern Instrument, U.K.) and a Rheometrics Mechanical Spectrometer 800 (Rheometrics, Inc.) over the

Table 3. Summary of Solids Concentrations and Complex and Relative Viscosities of Samples

	Solids Content (wt %)				Relative Viscosity		
temperature (K)	asphaltenes[a]	solid maltene	total solids	zero-shear complex viscosity (Pa s)	zero-solid	zero-asphaltene	chemically separated, maltene-based
				Sample ABP10			
298	5.3	19.6	24.9	185	2.58	0.989	30.1
323	5.3	0	5.3	5.63	0.776	0.777	8.78
348	5.3	0	5.3	0.683	0.671	0.670	2.85
373	5.3	0	5.3	0.189	1.02	1.02	2.70
				Sample ABP20			
298	10.4	18.5	28.9	426	5.93	2.28	69.4
323	10.4	0	10.4	11.7	1.61	1.61	18.3
348	10.4	0	10.4	1.20	1.18	1.18	5.00
373	10.4	0	10.4	0.244	1.31	1.31	3.48
				Sample ABP50			
298	13.6	17.9	31.5	458	6.38	2.45	74.6
323	13.6	0	13.6	11.9	1.64	1.64	18.6
348	13.6	0	13.6	1.13	1.11	1.11	4.71
373	13.6	0	13.6	0.305	1.64	1.64	4.35
				Sample AB (Bitumen)			
298	18.6	16.8	35.4	1710	23.8	9.14	279
303	18.6	13.4	32.0	581	13.2	6.81	161
323	18.6	0	18.6	32.4	4.47	4.47	50.5
348	18.6	0	18.6	2.72	2.67	2.67	11.3
373	18.6	0	18.6	0.507	2.73	2.73	7.23
				Sample ABR200			
298	50.0	10.3	60.3	8.84×10^8 [b]	1.23×10^7	4.73×10^6	1.44×10^8
323	50.0	0	50	1.00×10^6 [b]	1.38×10^5	1.38×10^5	1.56×10^6
348	50.0	0	50	6.98×10^3 [b]	6.85×10^3	6.84×10^3	2.91×10^4
373	50.0	0	50	3.20×10^2	1.72×10^3	1.72×10^3	4.56×10^3
				Sample ABR10			
323	57.2	0	57.2	7.50×10^5 [b]	1.03×10^5	1.03×10^5	1.17×10^6
373	57.2	0	57.2	3.80×10^2	2.04×10^3	2.04×10^3	5.42×10^3
				Sample MP5			
298	1.5	12.0	13.5	0.305	1.13	0.852	6.09
303	1.5	8.9	10.4	0.210	0.961	0.631	5.20
323	1.5	0.8	2.3	0.132	1.31	1.31	4.34
373	1.5	0	1.5	0.0120	0.574	0.574	
				Sample MP10			
298	6.2	11.4	17.6	0.506	1.88	1.41	10.1
303	6.2	8.4	14.6	0.318	1.45	0.955	7.87
323	6.2	0.8	6.9	0.142	1.41	1.41	4.67
373	6.2	0	6.2	0.0144	0.689	0.689	
				Sample MP20			
298	8.1	11.2	19.3	0.631	2.34	1.76	12.6
303	8.1	8.3	16.4	0.420	1.92	1.26	10.4
323	8.1	0.7	8.8	0.150	1.49	1.49	4.93
373	8.1	0	8.1	0.0166	0.794	0.794	
				Sample MP50			
298	9.4	11.0	20.4	0.879	3.26	2.46	17.5
303	9.4	8.2	17.5	0.445	2.04	1.34	11.0
323	9.4	0.7	10.1	0.170	1.69	1.69	5.59
373	9.4	0	9.4	0.0177	0.847	0.847	
				Maya Crude Sample			
298	15.7	10.2	25.9	0.954	3.54	2.66	19.0
303	15.7	7.6	23.3	0.701	3.21	2.11	17.4
323	15.7	0.7	16.4	0.225	2.23	2.23	7.40
348	15.7	0	15.7	0.079	1.82	1.82	3.00
373	15.7	0	15.7	0.039	1.87	1.87	
				Sample MR5			
323	46.7	0.4	47.1	6.87×10^4 [c]	6.82×10^5	6.82×10^5	2.26×10^6

[a] Phase angle and calorimetric measurements for neat asphaltenes suggest that, although the phase transitions to liquid begin at lower temperatures, asphaltenes are primarily solid up to a temperature of 373 K. [b] The zero-shear viscosity for these samples was obtained using the superposition approach. [c] For the MR5 retentate, viscosity was available at one temperature. This value was obtained at 0.01 Hz and is not a zero-shear value.

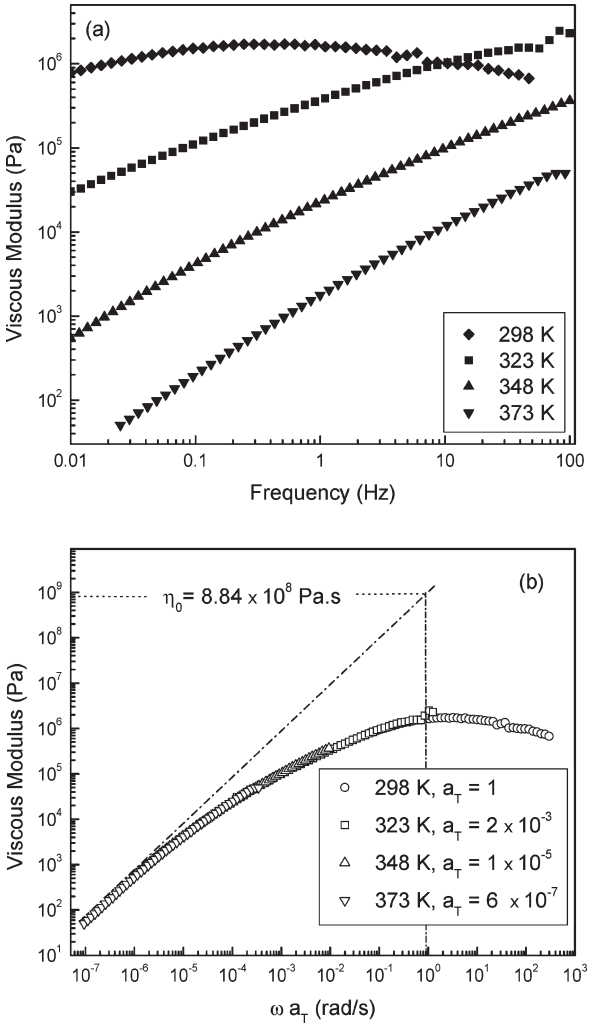

Figure 6. (a) Viscous modulus data for Athabasca bitumen, 200-nm retentate; (b) viscous modulus master curve used to estimate the zero-shear viscosity at 298 K (a_T is the shift factor).

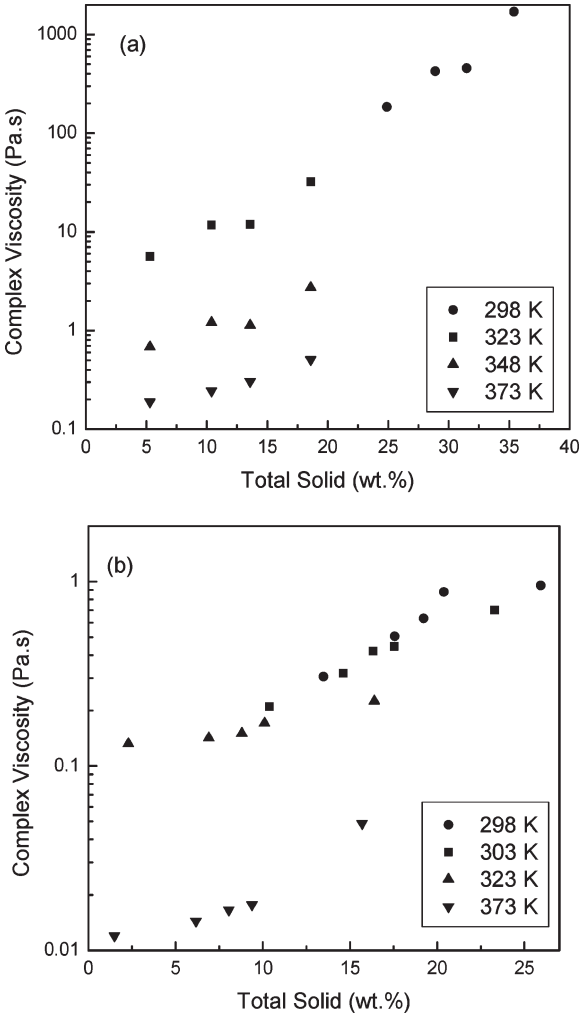

Figure 7. Zero-shear complex viscosity, as a function of sample solids content: (a) Athabasca bitumen-related samples and (b) Maya crude oil-related samples.

temperature range of 298−373 K. Complex viscosity, $|\eta^*(\omega)|$, is defined as

$$|\eta^*(\omega)|^2 = |\eta'(\omega)|^2 + |\eta''(\omega)|^2 \quad (2)$$

where $\eta'(\omega)$ is the dynamic viscosity ($\eta' = G''/\omega$), $\eta''(\omega)$ the imaginary part of complex viscosity resulting from the elastic component ($\eta'' = G'/\omega$), ω the angular frequency, G'' the loss (viscous) modulus, and G' the storage (elastic) modulus.

Two types of measuring configurations were used:

(1) (a) For Athabasca bitumen-related samples, parallel plate geometries with 25- and 40-mm-diameter plates supplied with the extended temperature cell of Malvern Instrument, providing a temperature range of 123−823 K with a stability of ±0.2 K, was used; (b) for some Maya crude-related samples, parallel plate geometries with 25- and 40-mm-diameter plates supplied with the Rheometrics Mechanical Spectrometer 800 were used.

(2) A double-gap 24/27-mm concentric cylinder with a Peltier cylinder assembly, allowing measurements over a range of 253−453 K with a stability of ±0.2 K was used for very-low-viscosity samples (e.g., the chemically separated Athabasca bitumen and Maya maltenes).

The thermocouple probe that reads the temperature of the bottom plate and hence indicates the temperature of the sample being sheared was calibrated to international temperature scale ITS 90 using a PT 100 resistance thermometer. The thermocouple in the Peltier cylinder was calibrated in the same way. In both cases, the uncertainty of temperature measurements was estimated to be ±0.2 K.

In the double-gap cylinder, the gap was fixed at the default value of 0.15 mm. For the parallel plate configuration, gaps of 0.85, 1.0, and 1.6 mm were applied for highly viscous samples (e.g., Athabasca bitumen and retentates), whereas gaps of 0.20 or 0.45 mm were used for samples with intermediate viscosities (1.0−500 Pa s). These gaps were chosen based on test measurements on three different standard materials: Canon certified standard N2700000SP, PRA standard oil 12, and PRA standard oil U0600. Viscosity measurements with the Canon certified viscosity standard N2700000SP (with a viscosity of 1650 Pa s at 310.5 K) were obtained to validate experimental conditions and parameter values selections for Athabasca bitumen. The conditions used for the Maya crude oil and permeates were validated using PRA standard oil 12 and PRA standard oil U0600 with viscosities of 0.972 and 0.1 Pa s at 298 K, respectively. The agreement with the recommended data was within 5%.

To ensure the consistency of the measurements obtained using different geometries, experiments were performed using more than geometry in the overlap range where geometries could be used interchangeably. Results agreed within experimental error. In some cases, experiments were repeated with more than one gap to ensure that the gap used was within appropriate limits. Artifacts related to "gap loading" were thus avoided.

Table 4. Zero-Shear Reference Viscosities

	Zero-Shear Reference Viscosity (Pa s)		
	Extrapolation		
temperature (K)	solid-free	0% asphaltenes	maltenes measurement (chemically separated)
		Athabasca Bitumen	
298	71.8	187	6.14
303	44.1	85.3	3.60
323	7.25	7.25	0.641
348	1.02	1.02	0.240
373	0.186	0.186	0.0701
		Maya Crude Oil	
298	0.270	0.358	0.0501
303	0.219	0.333	0.0404
323	0.101	0.101	0.0304
348	0.0434	0.0434	0.0266
373	0.0209	0.0209	

The measurements were performed using the oscillatory shear method. The frequency of the oscillation was varied between 0.0001 Hz and 100 Hz, depending on the sample. We use the term "frequency" in this paper, but it should be noted that the frequency of oscillation is equivalent to the term shear rate used in steady shear experiments, when both are expressed in the same units, i.e., the Cox−Merz rule ($|\eta^*(\omega)| = \eta(\dot{\gamma} = \omega)$) can be applied. All measurements were performed under nitrogen, to avoid oxidation of the samples. For all experiments, an oscillation amplitude sweep test was performed first, at the lowest and highest frequencies, to identify the stress and strain limits for the linear viscoelastic region, within which subsequent experiments were conducted.

Results and Discussion

1. Overview of Rheological Data for Athabasca Bitumen and Maya Crude Oil. The complex viscosity data obtained from oscillatory shear measurements at 298, 303, 323, 348, and 373 K are reported in Figures 2a and 2b for Athabasca bitumen and in Figure 2c for Maya crude oil. For low-viscosity samples, the inertia effect becomes significant at high frequencies, which causes fluctuation and scatter in measured data. Therefore, complex viscosity data for the frequency range of 0.1−100 Hz are only shown for highly viscous samples. Athabasca bitumen is ~3 orders of magnitude more viscous than Maya crude oil at 298 K. The viscosity of both materials is highly sensitive to temperature. An increase in temperature from 298 K to 373 K decreases the viscosity of Athabasca bitumen by 3 orders of magnitude and that of Maya crude by 2 orders of magnitude. Both Maya crude and Athabasca bitumen exhibit Newtonian plateaus at low shear rate over the entire temperature interval evaluated, although it is only evident at frequencies of < 0.01 Hz for Athabasca bitumen at 298 K (see Figure 2b).

Figure 3 shows a comparison between zero shear complex viscosity values of Athabasca bitumen obtained in this study with apparent viscosity values (η) that have been previously reported.[21−28] The complex viscosity values obtained in this study are higher, except for values obtained by Ward and Clark[24] (Abasand), Charbonnier et al.[22] (for some locations), and Camp[21] (Abasand). This is because zero shear viscosities, by definition, are the highest values, and because our bitumen sample is a partially processed product from a naphtha recovery unit at Syncrude. Some of the more volatile constituents of the bitumen have been removed. Differences in extraction and post-extraction processes, source location, measurement method, and measurement operating parameter differences[31] can all account for significant differences in the reported viscosity among samples.

2. Rheological Properties of Nanofiltered Permeates and Retentates. Rheological data for permeates at 298 K, the lowest temperature evaluated, are shown in Figures 4a for Athabasca bitumen permeates and 4b for Maya crude oil permeates. All permeates exhibit a Newtonian plateau at low frequency. Rheological data for retentates, at 323 K, are shown in Figure 5 for both Athabasca bitumen retentates and Maya crude oil retentates. The complex viscosity for the retentates increases as the frequency decreases. Such shear-dependent behavior at low frequencies is typically observed when a gel-type microstructure is present or when particles form a continuous network. At 298 K, Athabasca bitumen and Maya crude oil and their related permeates are both Newtonian; thus, a particulate network is the more logical explanation for this non-Newtonian behavior of retentate samples. These results lend support for a colloidal structure for hydrocarbon resources first suggested decades ago, without proof, by Nellensteyn.[54]

Zero-shear complex viscosity values for all permeate and retentate samples, along with the resource samples, are presented in Table 3. The zero-shear viscosity for some retentate samples could not be measured and was estimated using the superposition principle.[55] These are noted by a footnote in Table 3. If one takes into account the definition of complex viscosity described by eq 2, the viscous component dominates on the Newtonian plateau: $\eta^*(\omega) \approx \eta'(\omega) \approx \eta_0$. Therefore, the zero-shear viscosity (η_0) can be determined from the slope of the G'' vs ωa_T master curve (where a_T is a shift factor), which is constructed by shifting G'' curves at different temperatures along the ω-axis. G'' master curves were obtained for retentate samples where possible. Figure 6a shows the viscous modulus (G'') for the Athabasca bitumen, 200-nm retentate sample at different temperatures. The G'' master curve for this case, which illustrates the method for obtaining the zero-shear viscosity for the 200-nm retentate sample at 298 K, is shown in Figure 6b. A terminal zone (constant slope regime) is clearly visible at very low frequencies in the G'' master curve. A tangent line is drawn in the terminal zone of the master curve,

(54) Nellensteyn, F. J. *The Colloidal Structure of Bitumen,* Ph.D. Thesis, Delft Technical University, Delft, The Netherlands, 1923.
(55) Gurp, M. V.; Palmen, J. *Rheol. Bull.* **1998**, *67* (1), 5.

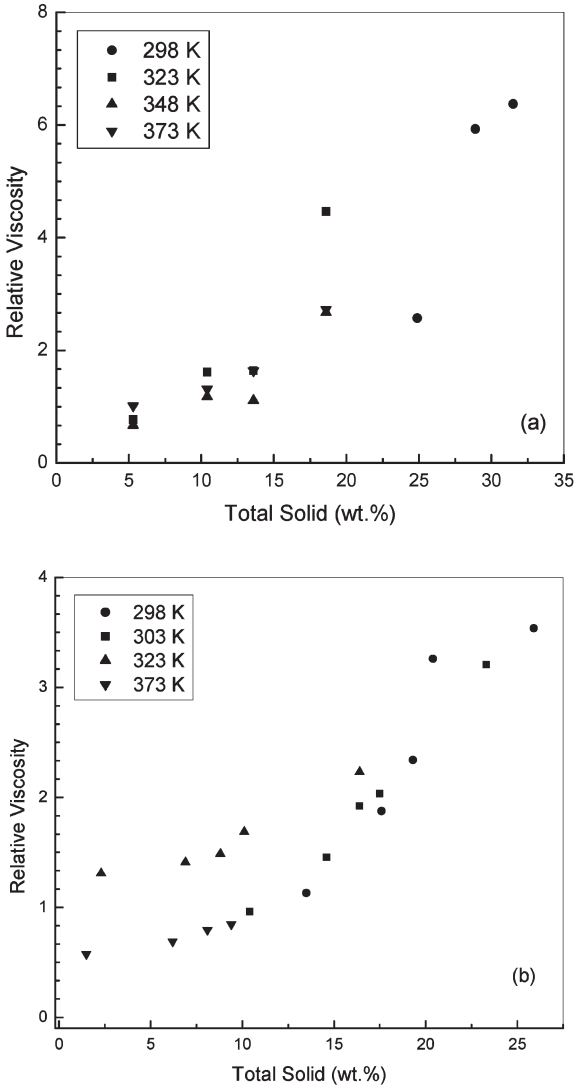

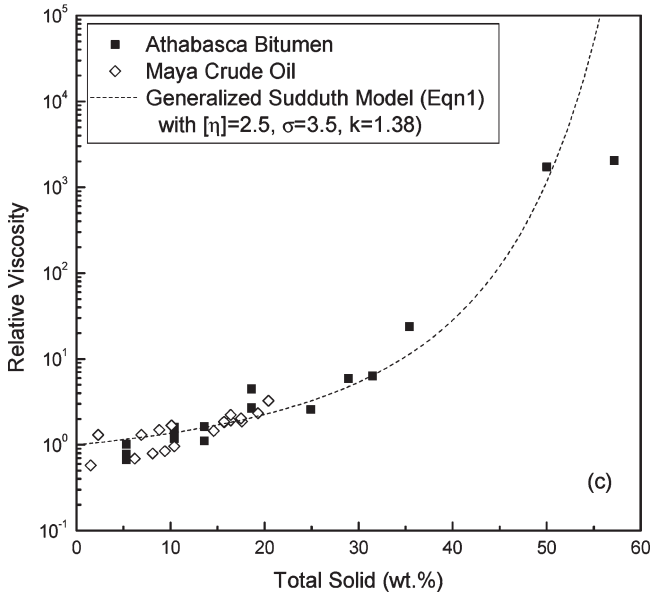

Figure 8. Zero-shear zero-solid relative viscosities: (a) Athabasca bitumen permeates, (b) Maya crude permeates, and (c) all data.

and this line is extended until it intersects the vertical line at $\omega a_T = 1$. The G'' value at this intersection point gives the zero-shear viscosity of the sample. A key assumption in this calculation is that the composition of the liquid is invariant. Because we are extrapolating into the low-temperature region, where part of the maltene solidifies, the values obtained are viewed as tentative and are not used in the modeling work.

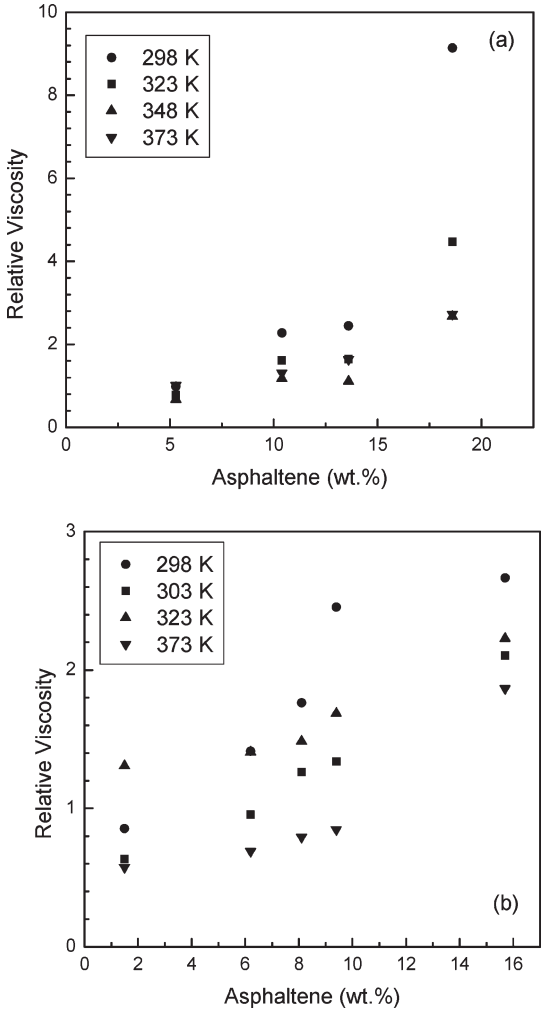

Figure 9. Zero-shear, zero-asphaltene relative viscosities: (a) Athabasca bitumen permeates and (b) Maya crude permeates.

3. Impact of Solid Maltenes on the Viscosity of Athabasca Bitumen and Maya Crude Oil. The solid−liquid transitions for both Athabasca bitumen and Maya crude oil maltenes occur over broad temperature ranges: ~160−325 K for Maya crude maltenes, and ~210−323 K for Athabasca bitumen maltenes.[45,46] With regard to the solids mass fraction, 16.8% and 10.2% of Athabasca bitumen and Maya crude maltenes, respectively, are solid at 298 K. Asphaltenes are also solid at 298 K, and the total solids mass fractions for Athabasca bitumen and Maya crude at 298 K are 35.4% and 25.9%, respectively, as shown in Figure 1. This effect complicates the interpretation of rheological data, because the solids content, solids density, and composition of the solid-free maltene in permeate, resource, and retentate samples, are functions of temperature at temperatures of <323 K. Calorimetric data[45,46] indicate that Maya and Athabasca asphaltenes begin to melt at ~340 K. However, the phase angle for pentane asphaltenes does not start to increase from 0° until ~380 K, which indicates that, up to this temperature, asphaltenes are comprised of a minimum of 65% solids. Moreover,

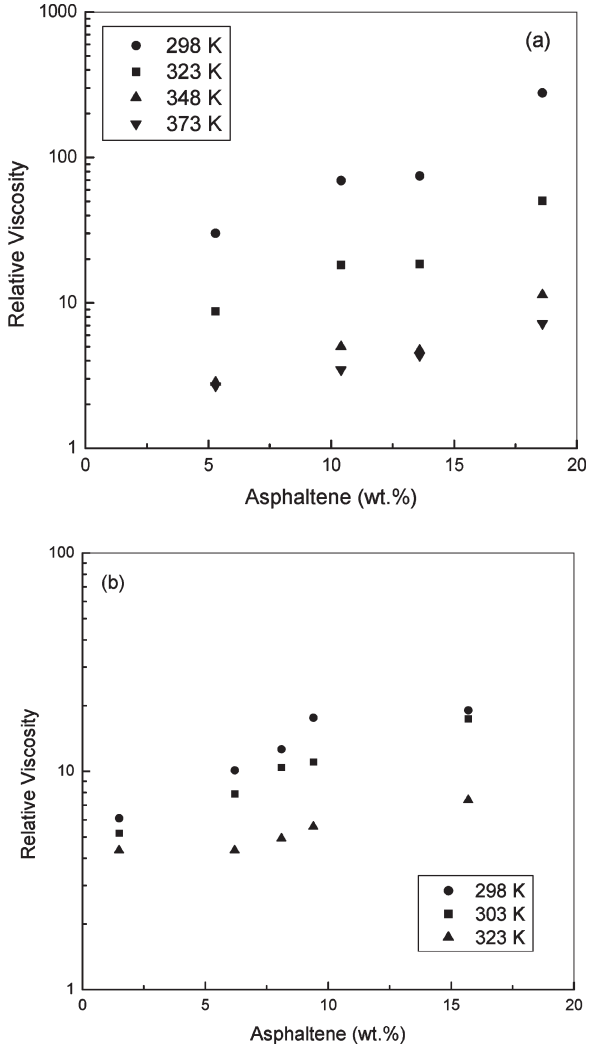

Figure 10. Zero-shear, chemically separated maltene-based relative viscosities: (a) Athabasca bitumen permeates and (b) Maya crude permeates.

asphaltenes remain filterable from maltenes at 473 K.[47] Clearly, liquid asphaltenes remain part of the dispersed solid asphaltene particles at 473 K. The structure of the two-phase region particles is unknown. In this study, we assume that the particles are solid continuously. The solid maltene, asphaltene, and total solids mass fraction, along with the zero-shear complex viscosities of samples, are summarized in Table 3. The zero-shear complex viscosities of permeate samples at different temperatures are reported in Figure 7a for Athabasca bitumen-related samples and Figure 7b) for Maya crude oil-related samples. A temperature dependence on the zero-shear complex viscosity is evident.

To estimate the viscosity of the solid-free Athabasca maltene and Maya crude oil maltene, the experimental viscosity values for permeates and resource samples were fitted with the generalized Sudduth model (eq 1) and the Arrhenius equation:

$$\eta_0 = A \exp\left(\frac{E}{RT}\right) \tag{3}$$

where A is the pre-exponential factor, E the activation energy of viscous flow for solid-free maltene, R the universal gas constant, and T the absolute temperature. Assuming the intrinsic viscosity to be given as $[\eta] = 2.5$ and the particle interaction coefficient to be given as $\sigma = 3.5$, the best fit was obtained for $k = 1.38$ with $A = 9.69 \times 10^{-12}$ Pa s and $E = 73.5$ kJ/mol for Athabasca bitumen samples, and $A = 8.05 \times 10^{-7}$ Pa s and $E = 31.5$ kJ/mol for Maya crude samples. The values of the activation energies are in good agreement with literature values.[56−61] Activation energies are in the range of 10−40 kJ/mol for low-viscosity samples and 60−80 kJ/mol for high-viscosity samples. For example, Ronningsen et al.[56] determined the activation energy of several North Sea crude oil samples with viscosities in the range of 3.7−155 mPa s (at 293 K), to lie in the range of 10−40 kJ/mol. For crude oils with viscosities in the range of 0.135−2.24 Pa s (at 293 K),[57] the activation energy was ∼20 kJ/mol. These samples have viscosities in the range of Maya crude oil, and their activation energies are similar to that of Maya crude oil. For the Cold Lake and Lloydminster oil samples, which have viscosities of ∼100 Pa s (at ∼295 K)[58] and 0.3 to 50 Pa s (at 293 K),[59] respectively, the activation energies are 80 and 60−80 kJ/mol, respectively. The activation energies and viscosities of these samples are similar to those of Athabasca bitumen.

The extrapolated solid-free maltene viscosity values for Athabasca bitumen and Maya crude oil are listed in Table 4. These viscosity values are higher than the viscosities of chemically separated maltenes, which are also shown in Table 4; this phenomenon may be due to the presence of residual solvent in the chemically separated maltene samples.

Experimental zero-solid relative viscosity values (which are defined as the zero-shear complex viscosity divided by the solid-free maltene viscosity) for the Athabasca bitumen and Maya crude oil samples, along with those of their permeates, are also shown in Table 3 and are plotted in Figures 8a and 8b, respectively. The zero-solid relative viscosities for all samples are shown in Figure 8c. The relative viscosities of all permeates, feeds, and retentate samples fall on a single master curve. Sudduth's correlation[53] (eq 1), with $[\eta] = 2.5$, $\sigma = 3.5$, and $k = 1.38$, is also shown in Figure 8c. There are two types of solids present; their individual densities are unknown a priori. Differences between the solids mass fraction and the solids volume fraction are accommodated in the value of the crowding factor, k, which is the only parameter that is adjusted in the model. Both types of solids are expected to be denser than the liquid maltenes. The crowding factor appears twice in eq 1; therefore, this represents a compromise. One could add additional parameters in the denominator for each feed but this is not justified by the data. The rheological behaviors of Athabasca bitumen and Maya crude oil feeds, retentates, and permeates are consistent with the behavior of slurries that are comprised of a Newtonian liquid plus rigid hard spheres in the temperature range of 298−373 K. Some of the relative viscosities fall below 1. This reflects the combined impact of experimental error and extrapolation to zero-solid content.

If the impact of solid maltene is ignored, one is confronted with significant apparent temperature dependences for relative

(56) Ronningsen, H. P.; Bjorndal, B.; Hansen, A. B.; Pedersen, W. B. *Energy Fuels* **1991**, *5* (6), 895.
(57) Kok, M. V.; Letoffe, J.; Claudy, P. *J. Therm. Anal. Calorim.* **1999**, *56*, 959.
(58) Bryan, J.; Kantzas, A.; Bellehumeur, C. *SPE Res. Eval. Eng.* **2005**, *8*, 44 (SPE Paper No. 89070).
(59) Luo, P.; Gu, Y. *Fuel* **2007**, *86*, 1069.
(60) Evdokimov, I. N.; Eliseev, N. Y.; Eliseev, D. Y. *Fuel* **2004**, *83* (7−8), 897.
(61) Evdokimov, I. N.; Eliseev, N. Y.; Eliseev, D. Y. *Fluid Phase Equilib.* **2003**, *212*, 269.

viscosities at fixed asphaltene mass fractions at temperatures where the maltenes are partially solid. For example, a zero-asphaltene reference viscosity can be obtained using eq 1, evaluated at the solid maltene mass fraction in a sample. Reference viscosities for this case are reported in Table 4, and the relative viscosity values obtained are plotted against the asphaltenes mass fraction in Figure 9. An apparent temperature dependence is evident for Athabasca bitumen-related samples (see Figure 9a). For Maya crude oil-related samples (Figure 9b), the impact is less pronounced, because less of the maltene is solid. An alternative relative viscosity can also be defined using measured chemically separated maltene viscosity as the reference viscosity. Reference viscosities for this case are also shown in Figure 4. Relative viscosities are reported in Table 3, and they plotted in Figures 10a for Athabasca bitumen-related samples and Figure 10b for Maya crude oil-related samples. Again, the apparent temperature dependence of rheological behavior is significant. These apparent temperature dependences have been attributed to changes in the shape of the asphaltene aggregates, the asphaltene−maltene interaction, or asphaltene self-association.[56,58,62] These seem to be misattributions, based on artifacts, and measured variables that introduce additional fluid physics and fluid chemistry that are not needed to explain the rheological behavior of such fluids. Rheological investigations of hydrocarbon resources must account for the impacts of solid maltenes and the asphaltenes in modeling and analysis.

(62) Lin, M.-S.; Chaffin, J. M.; Davison, R. R.; Glover, C. J.; Bullin, J. A. In *Structures and Dynamics of Asphaltenes*; Mullins, O. C., Sheu, E. Y., Eds.; Plenum Press: New York, 1998; p 267.

Conclusions

Hydrocarbon resources such as Athabasca bitumen and Maya crude oil possess complex phase behaviors and present equally complex rheological properties. The impact of non-asphaltenic solids on the complex viscosity of hydrocarbon resource samples at specific temperatures and on trends with temperature, is underscored in this contribution. Solid maltenes are shown to play a crucial role in determining the rheological properties of bitumen and heavy oil. Permeates, retentates, and feeds that are associated with nanofiltered Maya crude oil and Athabasca bitumen exhibit rheological behaviors that are consistent with slurries that are comprised of a Newtonian liquid and noninteracting hard spheres in the temperature range of 298−373 K when the role of solid maltenes is included. Failure to account for solid maltenes in the interpretation of rheological data for these hydrocarbon resources leads to misattributions that are related to the nature and importance of the role that asphaltenes play in the determination of hydrocarbon resource viscosity.

Acknowledgment. This research was supported by the Alberta Energy Research Institute, ConocoPhillips Inc., Imperial Oil Resources, Halliburton, Kellogg Brown and Root, NEXEN Inc., Shell Canada, Total, Virtual Materials Group, and the Natural Science and Engineering Research Council of Canada (NSERC). The authors appreciate the help of Bei Zhao in nanofiltered sample preparation, and they thank Mildred Becerra for technical assistance in the lab. The Nanotechnology Scholarship of the Alberta Ingenuity Fund and FS Chia PhD Scholarship from the Faculty of Graduate Studies and Research, University of Alberta for A.H. are also gratefully acknowledged.